Immunity, Volume *37*

Supplemental Information

Commensal Bacteria Calibrate the Activation Threshold of Innate Antiviral Immunity

Michael C. Abt, Lisa C. Osborne, Laurel A. Monticelli, Travis A. Doering, Theresa Alenghat, Gregory F. Sonnenberg, Michael A Paley, Marcelo Antenus, Katie L. Williams, Jan Erikson, E. John Wherry, and David Artis

Supplemental Figure 1. related to Figure 1.

Additional analysis of viral persistence in the kidney and the LCMV-specific $CD8^+$ T cell response to multiple epitopes.

Supplemental Figure 2. related to Figure 2.

Contains data demonstrating effectiveness of antibiotic treatment in reducing commensal bacterial communities in the gastrointestinal tract and upper respiratory tract. Provides histology of lung from naïve CNV or ABX mice for comparison to Figure 2E-J. Contains data supporting histologic observation of increased epithelial cell death in the lung of ABX mice at d12 post-infection. Compares influenza virus infection in CNV and germfree (GF) mice.

Supplemental Figure 3. related to Figure 3.

Contains data demonstrating impaired immunity and increased susceptibility of ABX mice following infection with the weakly pathogenic X31-GP33 influenza virus strain.

Supplemental Figure 4. related to Figure 4

Consists of activation profile of plasmacytoid dendritic cells from CNV or ABX mice at d3 post influenza virus infection, expression of IL-10 in CNV or ABX mice prior to or following viral infection, and inflammatory cytokine and chemokines protein data supporting qPCR data shown in Figure 4D,E.

Supplemental Figure 5. related to Figure 5

Phenotypic profile of peritoneal macrophages and dendritic cells from naïve CNV or ABX mice

Supplemental Figure 6. related to Figure 5

Additional analysis of microarray data presented in Figure 5. Gene set enrichment analysis, gene expression of inflammasome and TLR signaling components, and qPCR analysis of antiviral defense genes.

Supplemental Figure 7. related to Figure 6

Contains data demonstrating IFN-γ and IFN-β responsiveness of macrophages isolated from CNV or GF mice and ability of macrophages to control viral replication *in vitro.*

Supplemental Table 1. related to Figure 3

Frequency of DbGP33 tetramer^{+} CD8^{+} T cells isolated from the lung of CNV or ABX mice expressing activation molecules at d7, 10, 12 post influenza virus infection

Supplemental Figure Legends

Figure S1. ABX mice exhibit a functionally impaired $CD8^+$ T cell response and persisting viral reservoirs following LCMV T1b infection. (A) Viral load in the kidney of CNV or ABX mice at d31 post-infection. (B) Splenocytes from d31 infected mice were either stained with H2-DbGP33, H2-DbGP276, or H2-DbNP396 tetramers or incubated with LCMV peptides (GP33-41, GP276-286, NP396-404) for 5 hrs in the presence of BFA and assessed for production of IFN-γ and TNF-α. Total number of DbNP396, DbGP33 or DbGP276 $tetramer^+$ $CD8^+$ T cells producing IFN-γ, IFN-γ and TNF-α, or no cytokines. (C) Total number of IFN-γ^+/TNF-α^+ dual producing $CD8^+$ T cells in the spleen at d31 post-infection following 5hr stimulation with a pool of 20 LCMV-specific peptides (Kotturi et al., 2007). Data representative of two independent experiments with n=4-5 mice per group. Data shown are mean $\pm$ SEM. *$p<0.05$, **$p<0.01$.

Figure S2. Absence or antibiotic-mediated disruption of commensal bacterial communities in the upper respiratory and gastrointestinal tract result in increased morbidity and impaired viral clearance following influenza virus infection. Culturable bacteria from (A) fecal samples or (B) trachea homogenates of naïve CNV or ABX mice. Samples were plated on LB agar and incubated for 48hrs in aerobic or anaerobic conditions (L.o.D. - limit of detection). (C) H&E stained lung sections from naïve CNV or ABX mice (scale bar: 200μm). (D) Flow cytometric analysis and (E) frequency of dead cells in the BAL fluid of CNV or ABX at d12 post-infection as assessed by an amine reactive viability dye. (F-J) CNV or GF C57BL/6 mice were infected i.n. with 368 $TCID_{50}$ recombinant influenza virus (PR8-GP33 strain). (F) Timecourse of weight loss following infection. (G) Influenza virus genome copies in the lung at d12 post-infection assessed by qPCR and displayed as $TCID_{50}$/gram of lung tissue

based on a standard curve of genome copies versus $TCID_{50}$. (H) Influenza virus-specific IgM and IgG antibody titers in serum at d12 post-infection. H&E stained lung sections of (I) CNV or (J) GF mice at d12 post infection. Black arrows highlight bronchiole epithelial necrosis and degeneration (scale bar: 50μm). Data representative of two independent experiments with n=3-4 mice per group. Viral titer statistics determined by Two-part *t*-test. Data shown are mean $\pm$ SEM. *p<0.05, **p <0.01.

Figure S3. ABX mice display an impaired influenza virus-specific $CD8^+$ T cell response and are susceptible to the weakly pathogenic X31-GP33 influenza virus. CNV or ABX C57BL/6 mice were infected i.n. with $1x10^5$ $TCID_{50}$ recombinant influenza virus X31-GP33. (A) Timecourse of weight loss following infection. (B) Influenza virus genome copies in the lung at d7 post-infection assessed by qPCR and displayed as $TCID_{50}$/gram of lung tissue based on a standard curve of genome copies versus $TCID_{50}$. (C) H&E stained lung section of CNV or ABX lungs at d7 post-infection (black arrow highlights epithelial necrosis and degeneration; scale 20μm). (D) Survival curve following infection. (E-H) Total number of DbGP33 tetramer$^+$ $CD8^+$ T cells in the (E) BAL, (F) lung, (G) mediastinal lymph nodes, and (H) spleen at d7 post-infection. (I) Lung cells were stimulated with GP33 peptide for 5hrs in the presence of BFA. Proportion of GP33 peptide responsive $CD8^+$ T cells in the lung producing multiple effector molecules (IFN-γ, TNF-α, IL-2, MIP-1α, CD107a). Data representative of three independent experiments with n=4-5 mice per group. Survival curve statistics determined by logrank test. Viral titer statistics determined by Two-part *t*-test. Data shown are mean $\pm$ SEM. *p<0.05, **p <0.01, ***p<0.001.

Figure S4. Reduced proinflammatory cytokine and chemokine production in ABX mice early following influenza virus or LCMV infection. (A) Absolute number of plasmacytoid dendritic cells (pDCs) in the lung at steady-state or d3 post influenza virus infection (PR8-

GP33). (B) Expression of CD40, CD86 and MHC-I on pDCs at d3 post-infection. FACS analysis excluded T cells ($CD3\varepsilon^+$), B cells ($CD19^+$), NK cells ($NK1.1^+$), alveolar macrophages, ($F4/80^+$, $CD11c^+$), conventional DCs ($CD11c^{hi}$, MHC-II^{hi}), inflammatory monocytes ($Ly6c^+$, $CD11b^+$), and neutrophils ($Ly6g^+$ $CD11b^+$) then gated on $CD11c^{mid}$, PDCA-1^+ cells to assess pDC expression of costimulatory molecules. (C,D) Relative expression of *Il10* mRNA in the (C) spleen or (D) lung of naïve CNV or ABX mice. (E) IL-10 protein present in the BAL fluid of influenza virus infected CNV or ABX mice (PR8-GP33). IL-10 levels determined by luminex multiplex bead array. Statistical analysis of individual timepoints was done by Student's *t*-test. (F) Proinflammatory cytokines and chemokines present in BAL fluid d3 post influenza virus infection. (G) Proinflammatory cytokine levels in spleen homogenates at 6-24hr post LCMV T1b infection (i.v.) (n.d. - not detectable). Data representative of two independent experiments with n=3-5 mice per group. Data shown are mean ± SEM. *p<0.05, **p<0.01.

Figure S5. Macrophages isolated from ABX mice have reduced expression of activation molecules at steady-state. Phenotypic characterization of (A) macrophages or (B) dendritic cells isolated from the peritoneal cavity of naïve CNV (black line) or ABX (red line) mice. Shaded histogram represents isotype control (or FMO for MHC-I and TLR-9). FACS plots gated on live, $CD45^+$, non-T, non- B, non-NK cells. Data representative of three independent experiments. Data shown are mean ± SEM. n=4-5 mice per group. *p<0.05, **p<0.01, ***p<0.001.

Figure S6. Macrophages isolated from CNV mice have increased expression of IFN response gene relative to macrophages isolated from ABX mice. (A) Heat map of differentially expressed genes in macrophages isolated from CNV or ABX mice. Red = high expression, blue = low expression. (B) Gene set enrichment analysis (GSEA) of CNV

macrophages compared to macrophages isolated from ABX mice. The most highly enriched gene sets determined by the normalized enrichment score (NES). (C) Enrichment curve of the top ranked gene set as defined by GSEA. (D) GSEA enrichment curve of genes upregulated following IFN-α stimulation, empirically defined from (Agarwal et al., 2009). Heat map of genes encoding (E) inflammasome components or (F) TLR signaling components in macrophages isolated from naïve CNV or ABX mice. (G) qPCR analysis of RNA isolated from sort-purified macrophages from two independent experiments with n=3-5 mice per group. Data shown are mean $\pm$ SEM. *p<0.05, **p<0.01.

Figure S7. Macrophages isolated from naïve GF mice have diminished ability to respond to IFN stimulation and control viral replication. Peritoneal macrophages isolated from naïve CNV or GF Swiss/Webster mice were stimulated with IFN-γ or IFN-β *in vitro*. Histograms of STAT1 phosphorylation in macrophages following (A) IFN-γ (0.2, 2, 20, 200ng/mL) or (C) IFN-β (10^1, 10^2, 10^3, 10^4 Units/mL) stimulation for 15 minutes. Mean florescence intensity (MFI) of pSTAT1 in macrophages following (B) IFN-γ or (D) IFN-β stimulation. (E) LCMV viral titers in supernatant of *in vitro* infected macrophages isolated from naïve CNV or GF mice at 24-72 hrs post-infection. (LCMV cl-13 strain, MOI of 0.2). Data representative of two independent experiments; n=3-5 mice per group. Data shown are mean $\pm$ SEM. **p<0.01, ***p <0.001.

Table S1. Frequency of DbGP33 tetramer$^+$ CD8$^+$ T cells that express CD69, CD25, Granzyme-b, CD43 or CXCR3 at d7, 10, or 12 post influenza virus infection (PR8-GP33 strain). Positive gate determined by expression of markers on naïve CD44^{lo} CD62L^{hi} CD8$^+$ T cells. Data shown are the mean $\pm$ SEM. *p<0.05, **p<0.01, ***p<0.001.

Supplemental Experimental Procedure

RNA isolation, cDNA preparation, and RT-PCR

RNA was isolated from cells using an RNeasy mini-kit (Qiagen) and from lung or spleen tissue using mechanical homogenization and TRIzol isolation (Invitrogen) according to the manufacturer's instructions. cDNA was generated using SuperScript reverse transcriptase (Invitrogen). RT-PCR was performed on cDNA using SYBR green chemistry (Applied Biosystems) and commercially available primer sets (Qiagen). PA influenza-specific primers and probes (Sense: CGGTCCAAATTCCTGCTGAT; Anti-Sense: CATTGGGTTCCTTCCATCCA; Probe: CCAAGTCATGAAGGAGAGGGAATACCGCT) were used to determine influenza virus genome copies based on a standard curve then converted to $TCID_{50}$/ gram of lung tissue. Genes of interest were normalized to *Actb* (or *Hprt* for whole spleen tissue) and displayed as fold difference relative to uninfected CNV control mice.

Virus-specific antibody and cytokine ELISA

LCMV or 1,000 HAU/mL of purified PR8 virus was adsorbed to plates and bound antibody from serum was detected using anti-IgM or -IgG conjugated to alkaline phosphatase (Sigma) and developed with *p*-nitrophenol phosphate (Sigma). PR8 antibody concentrations were determined using anti-HA antibody standards of IgM (clone H35-C7-2R1) or IgG (clone H36-4-5.2). Optical densities ($OD_{405-750}$) were measured using an ELISA reader and concentrations calculated using SoftMax Pro software (Molecular Devices). BAL wash supernatant and serum samples were analyzed for cytokines and chemokines by luminex multiplex bead array (Millipore). Tissue from the spleen was mechanically homogenized in DMEM, centrifuged, and the resultant supernatant was measured for cytokine secretion by ELISA (eBioscience). IFN-β

protein levels in the serum or spleen homogenates were measured by ELISA (PBL Interferonsource).

Fecal and tracheal bacterial culture

Stool pellets were collected 2 weeks following antibiotic treatment, homogenized in PBS, and plated on Schaedler's agar by serial dilution and incubated at 37°C under aerobic or anaerobic conditions for 48 hours. Trachea tissue segment was isolated under sterile conditions by a board-certified Otolaryngologist with particular attention to ensure the trachea sample was separated from the esophagus. An approximate 2-3 cm portion of the trachea from the bottom of the larynx to where the trachea splits into the bronchioli was removed and mechanically homogenized in PBS. The resultant homogenate was plated by serial dilution on LB agar plates and grown under aerobic or anaerobic conditions for 48 hours.

Supplemental References

Agarwal, P., Raghavan, A., Nandiwada, S.L., Curtsinger, J.M., Bohjanen, P.R., Mueller, D.L., and Mescher, M.F. (2009). Gene regulation and chromatin remodeling by IL-12 and type I IFN in programming for CD8 T cell effector function and memory. J Immunol *183*, 1695-1704.

Kotturi, M.F., Peters, B., Buendia-Laysa, F., Jr., Sidney, J., Oseroff, C., Botten, J., Grey, H., Buchmeier, M.J., and Sette, A. (2007). The CD8+ T-cell response to lymphocytic choriomeningitis virus involves the L antigen: uncovering new tricks for an old virus. J Virol *81*, 4928-4940.

Supplemental Figure 1

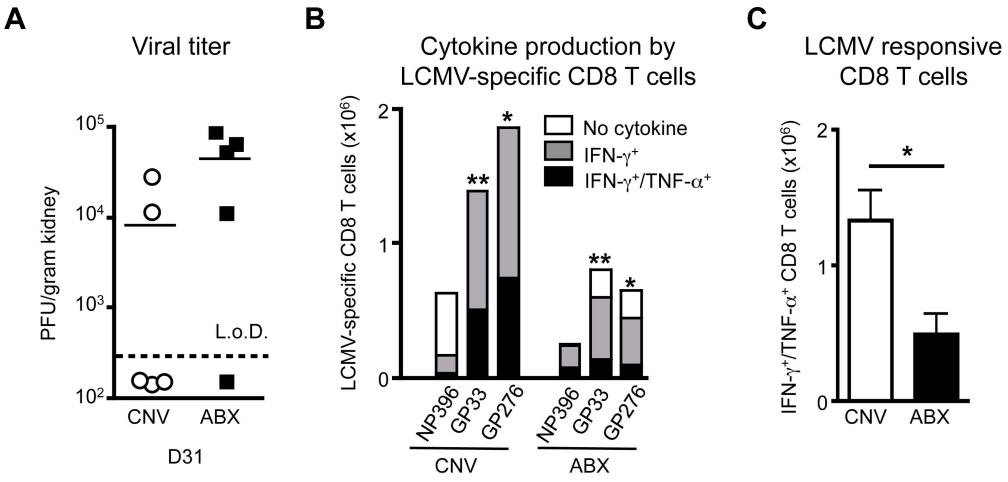

Supplemental Figure 2

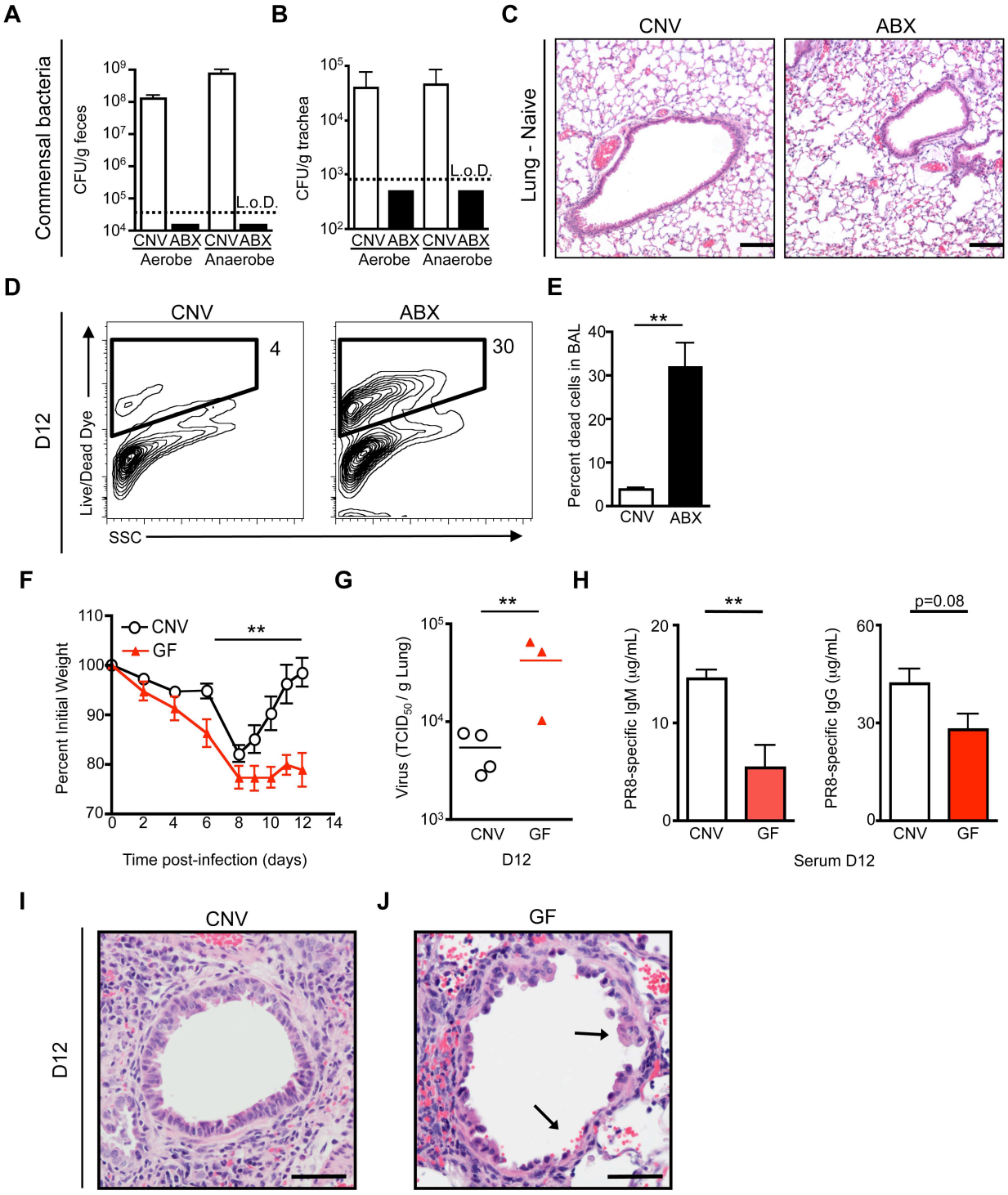

Supplemental Figure 3

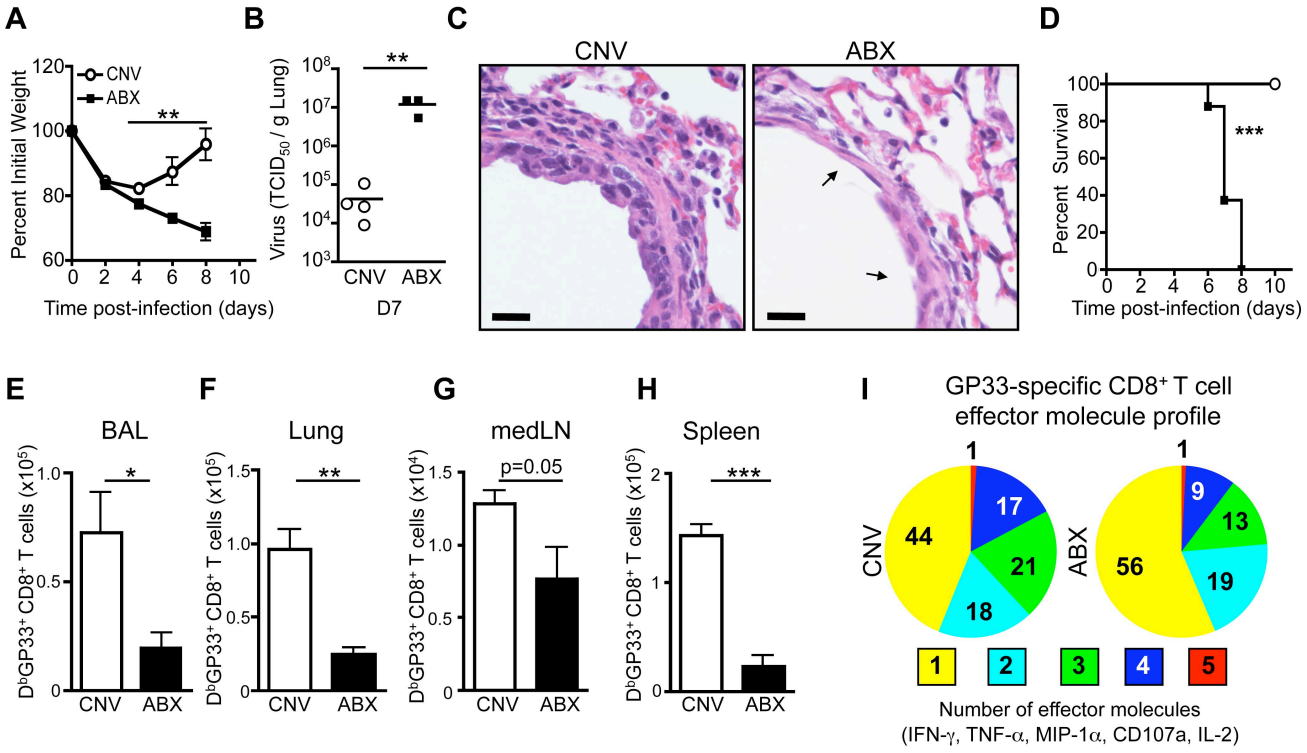

Supplemental Figure 4

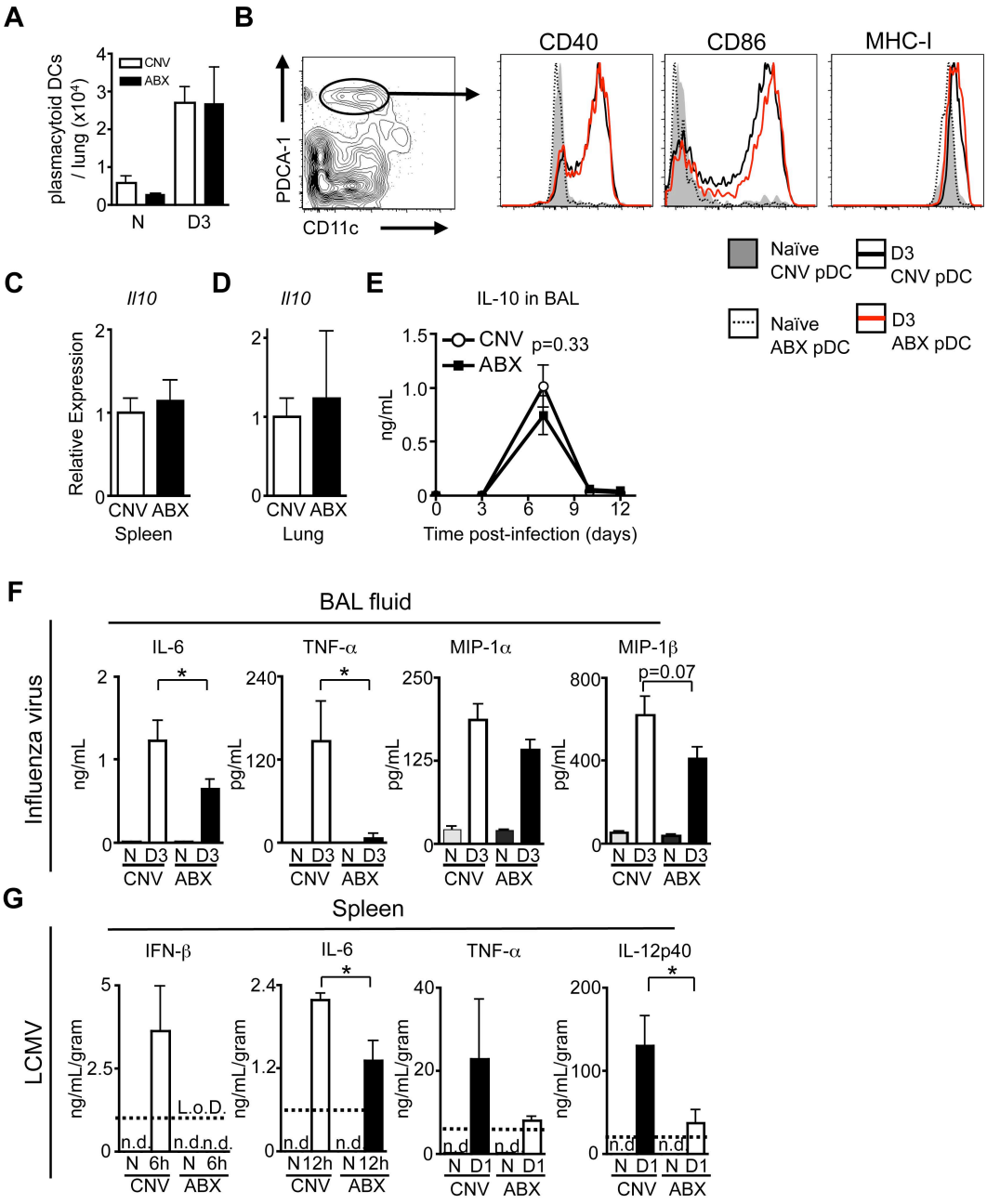

Supplemental Figure 5

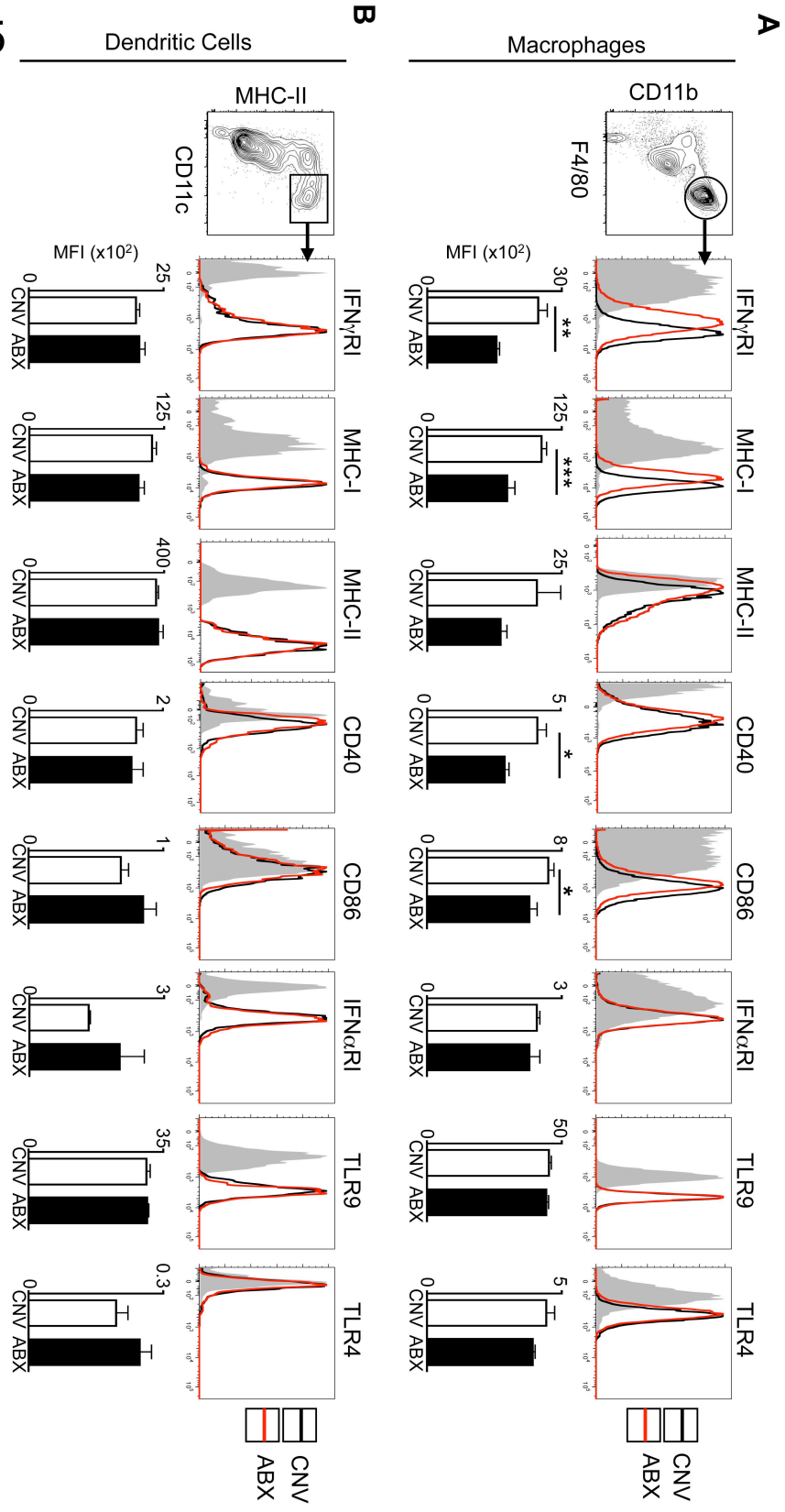

Supplemental Figure 6

A

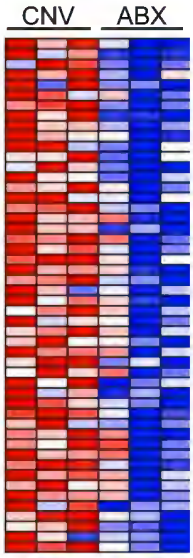

B

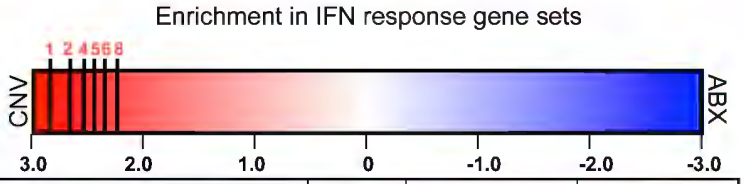

NAME	NES	NOM p-val	FDR q-val
1. IFN RESPONSE GENES	2.77	<0.001	<0.001
2. IFN A RESPONSE	2.63	<0.001	<0.001
3. STAT3 TARGET DN	2.58	<0.001	<0.001
4. IFN A RESPONSE UP	2.50	<0.001	<0.001
5. IFN B RESPONSE UP	2.48	<0.001	<0.001
6. IFN SIG IN CANCER	2.45	<0.001	<0.001
7. TARGET NUP98 HOXA9	2.40	<0.001	<0.001
8. IFN RESPONSE	2.39	<0.001	<0.001

C

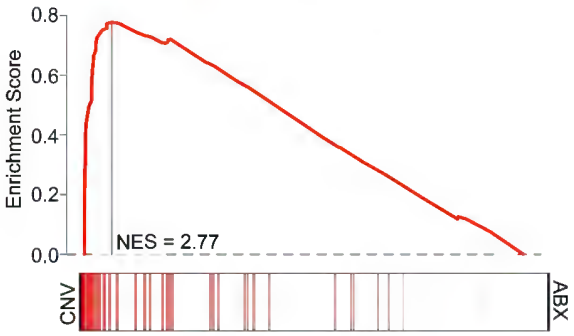

D

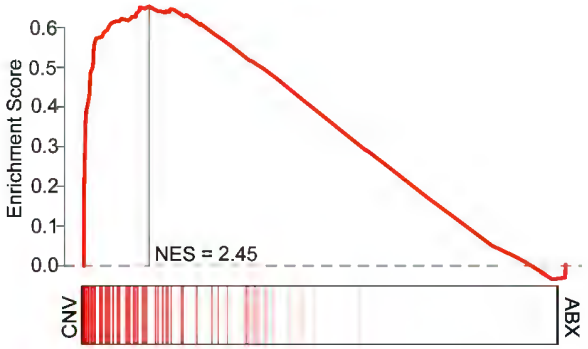

E

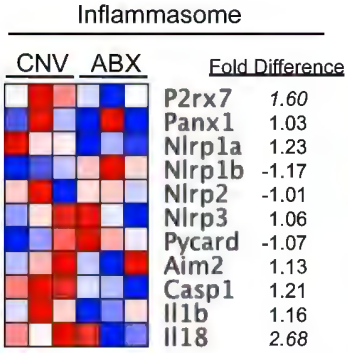

F

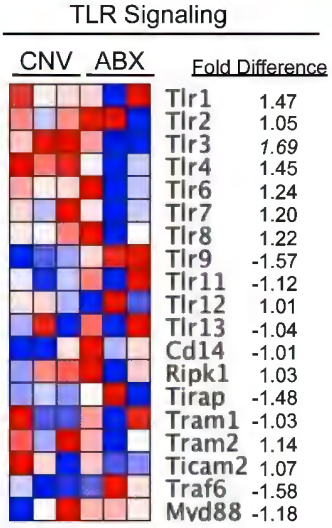

G

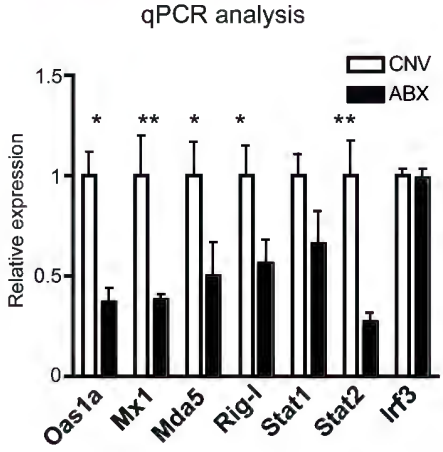

Supplemental Figure 7

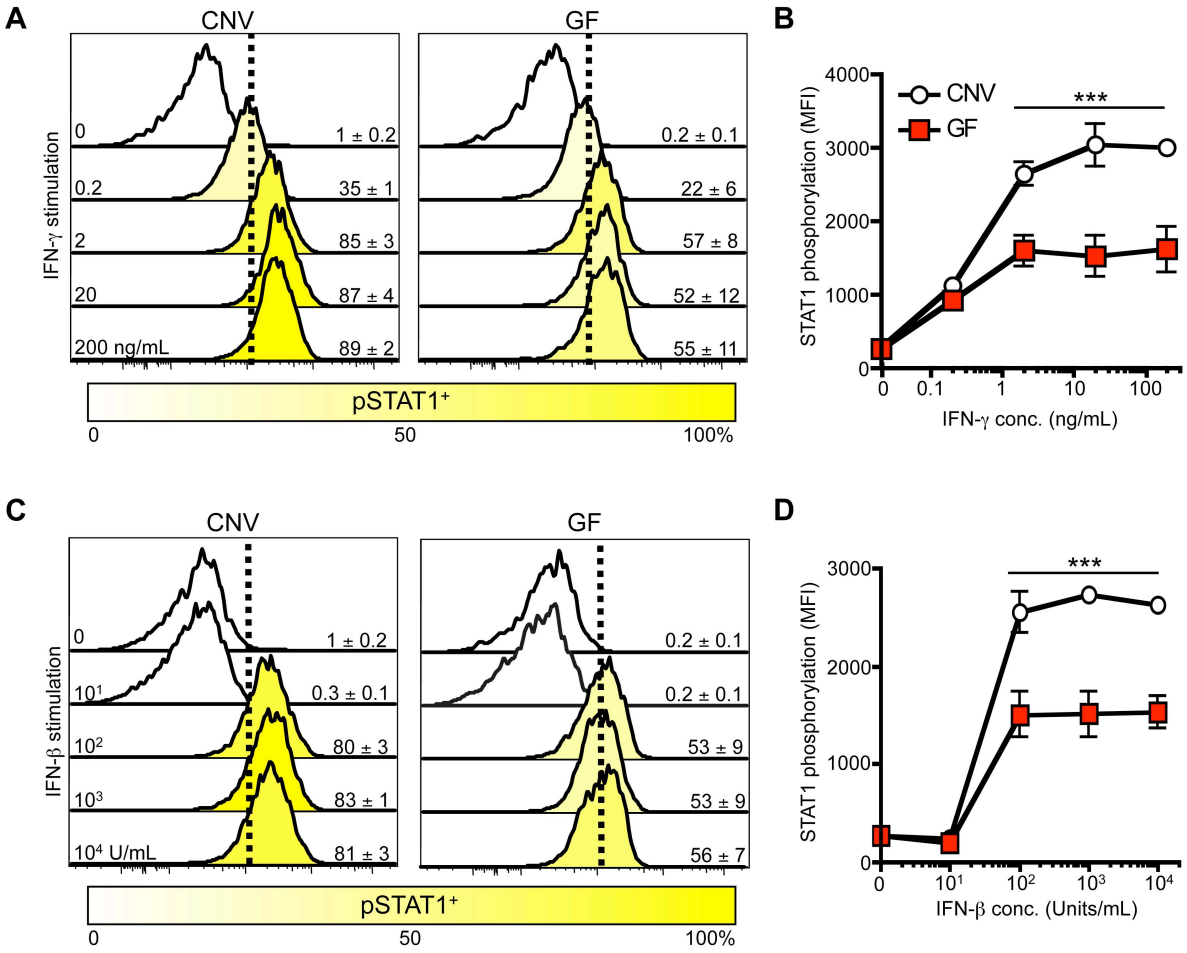

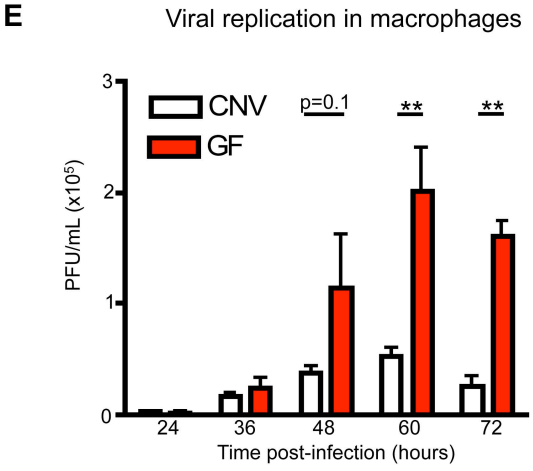

Supplemental Table 1: Lung D^bGP33 tetramer$^+$ $CD8^+$ T cells

Day		CD69$^+$	CD25$^+$	Gzmb$^+$	CD43$^+$	CXCR3$^+$
7	**CNV**	67.9 ± 3.9*	67.4 ± 3.4**	93.8 ± 3.9	94.6 ± 4.6	1.7 ± 0.4
	ABX	79.1 ± 6.7*	80.7 ± 2.3**	94.2 ± 3.4	94.6 ± 3.1	2.4 ± 2.8
10	**CNV**	58.5 ± 2.3	18.3 ± 6.4**	76.2 ± 5.4***	87.5 ± 3.8	34.2 ± 6.5**
	ABX	63.2 ± 4.3	35.5 ± 6.5**	96.5 ± 0.1***	90.0 ± 3.4	17.9 ± 2.5**
12	**CNV**	32.3 ± 4.5	11.4 ± 2.4	55.7 ± 4.8***	89.0 ± 4.2	16.8 ± 5.2
	ABX	30.7 ± 5.7	34.6 ± 11.7	84.5 ± 1.4***	90.6 ± 4.1	10.4 ± 0.3